IOP Conf. Series: Materials Science and Engineering **255** (2017) 012016 doi:10.1088/1757-899X/255/1/012016

On the Static Accuracy of Charge-Discharge Units Intended for Electrical Tests of High Capacity Li-ion Batteries

E A Mizrah, D K Lobanov, E A Kopylov, R V Balakirev, A S Fedchenko
Reshetnev Siberian State University of Science and Technology
31, Krasnoyarskiy rabochiy ave., Krasnoyarsk, 660014, Russia

E-mail: enis-home@mail.ru

Abstract. Performing of the cycle testing according to the principles of Dynamic Stress Test can significantly reduce the overall time of development and production of batteries, which in turn allows reducing the cost of designing and testing of the spacecraft power systems. Performing of Dynamic Stress Test require special charge-discharge units that allows to perform a full cycle of electrical tests of batteries, including cyclic testing. Providing the required accuracy of measurement and stabilization of certain attributes of Li-ion battery operating modes is one of the problems that arise during the development of such charge-discharge units. The following attributes are of particular interest: charge and discharge currents, discharge powers, battery voltages. Analysis of the charge-discharge unit as a control system allows evaluating the steady-state stabilization error of the required attributes of the developed device. Moreover, using a digital integrator in the control system of the charge-discharge unit allows providing specified values of steady-state stabilization error of required attributes in different test modes.

1. Introduction

Li-ion batteries are widely used in spacecraft power systems. Characteristics of Li-ion batteries significantly affect the spacecraft life cycle in orbit. Electrical tests of Li-ion batteries are performed during development and production at the factory, in particular, the battery cycle life is estimated by special designed cycle tests. These tests include multiple charge/discharge cycles in order to reduce total capacity and power of the batteries to a minimum value.

Reducing the time of the cyclic tests can significantly speed up and reduce the cost of designing and testing of spacecraft power systems. In order to reduce the duration of cyclic tests were developed methods of cycle tests for Li-ion batteries based on the method of Dynamic Stress Test (DST) [1–3]. This method involves increasing of charge-discharge currents of the tested battery up to the maximum values, including modes of discharging by constant power. Charging of batteries is typically performed according to the manufacturer's methods, discharging - by the techniques of DST.

There are many types of charge-discharge units (CDU) for Li-ion batteries [4–8], but these devices are not suitable for testing (including cycle testing) of isolated battery cells that have relatively low voltage and high capacity. There are also devices that allow testing of composite Li-ion batteries [9–10]. The disadvantages of the devices listed above include:

- input current of converter is not high enough: testing of batteries with rated capacity of 90 Ah requires current more than 100 A, which require using of multiple parallel connected devices;
- lack of opportunity to discharge battery to a negative voltage (polarity reversal), which does not allow to study the operation of the battery cells in the emergency situations..

2. Charge-discharge unit description

An automated CDU [11–12] (fig.1.) allows performing a full cycle of electrical tests.

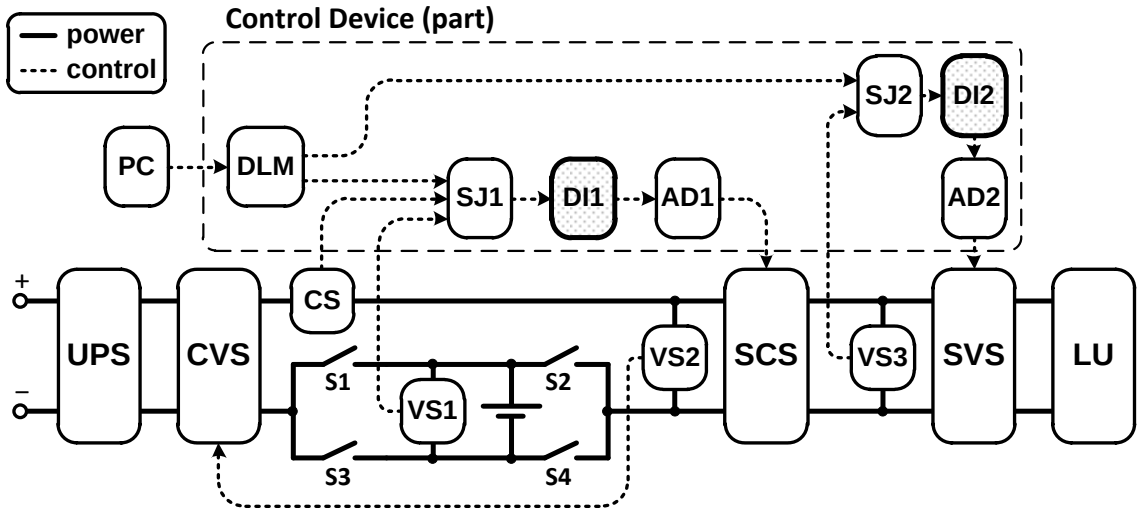

Figure 1. Block diagram of charge-discharge unit (CDU)

Uninterruptible power supply (UPS) prevents interruption of the tests in the case of emergency AC network shutdown. Charging and discharging modes of the battery are provided by appropriate position of switches S1-S4 and by a controlled voltage stabilizer (CVS). CVS allows ensuring stable charge/discharge mode operation. Excess of energy, consumed by CDU, is dissipated by a load unit (LU).

Necessity of current regulation in the wide range (0..160 A), the need for electrical isolation between switches S1-S4 and LU and complexity of high-frequency power transformer made it necessary to use two more stabilizers switched-mode stabilizer current (SCS) and switched-mode stabilizer voltage (SVS). SCS stabilizes its own input current, SVS stabilizes the SCS output voltage. SCS consist of switched-mode current regulator, which is based on boost converter. SVS consist of switched-mode voltage regulator, which is based on full-bridge buck converter.[13-14]

In order to provide high currents at low battery voltages it is necessary to maintain the SVS input voltage at the relatively high level. For this reason the stabilization of the SCS input voltage is provided by CVS (voltage sensor VS2 forms feedback for CVS). Therefore, regardless of battery voltage and the operating mode (charging or discharging of the battery) CVS stabilizes the SCS input voltage at the level of 4 V. In addition, the stabilization of the SCS input voltage enables to discharge the battery until polarity reversal.

A control device (CD), in accordance with predetermined patterns and the measured values of battery voltages and currents, controls switches S1-S4 (control routes between CD and switches are not shown on the diagram), generates control signals for SCS and SVS, and

provides safe completion of tests if charge of the UPS batteries is low and if voltage in AC network is absent. CD includes digital logic module (DLM) which connected to personal computer (PC) and forms references for SCS and SVS summing junctions (SJ) on which they are added to the signals from the current (CS) and voltage (VS1, VS3) sensors. Control signals for SCS and SVS are filtered by digital integrators (DI) (detailed description will be given below) and amplified by analog drivers (AD).

CDU performs following functions:

- stabilization and regulation of charge and discharge currents;
- stabilization and regulation of discharge power;
- reproduction of electrical and temporal operational modes of battery;
- automatic diagnostics of CDU condition;
- emergency operation protection.

Document [15] gives guidelines for the definition of performance characteristics, guidelines for Li-ion battery cycle testing, and recommended measurement errors for battery parameters which are:

a) ± 0.1% for voltages;
b) ± 1% for currents;
c) ± 0.1% for temporal parameters.

At the same time, document [15] does not establish requirements for the stabilization accuracy of charge and discharge currents and discharge powers. In accordance with the adopted in the design of control systems practice, take attributes stabilization errors equal to measurement errors:

a) ± 1% for currents;
b) ± 0.1% for temporal parameters;
c) ± 1.1% for power.

Providing the required current measurement accuracy is achieved by using high-precision current sensor and by current sensor calibration. Calibration of current sensors performs at the intervals specified in the automatic battery testing program and automatically before startup. Calibration allows reducing to a minimum the statistical component of the current sensor error.

Measurement of the battery voltage and voltages of current sensors is performed using specialized measuring device based on National Instruments modules. Since the electrical isolation of measurement channels is required, NI PXIe-4300 modules are used [16]. They provide 8 channels, which allow simultaneously measuring, and have percentage errors of measurement no more than 0.0245%.

Stabilization and control of the attributes is based on digital signal processing in the single-chip computer. Accuracy of stabilization consists of the sum of the errors:

- the current and voltage measurement errors (discussed above);
- errors caused by the analog-digital converter (ADC);
- errors caused by of the reference voltage source;
- errors of attributes stabilization control loops.

Errors of the ADC and reference voltage are minimized by selecting appropriate electronic components. Charge-discharge unit, described by the authors in [11-12], contains a switching regulator of the input current (SRIC) and a switching regulator of the SRIC output voltage (SRSOV).

3. Mathematical model

The mathematical model of the power part of CDU is based on the block diagram (fig. 1) and the equivalent circuit (fig. 2). This model allows analyzing the accuracy of CDU static stabilization.

Variations of voltages and currents in circuits are negligible in steady state, which allows omitting the parameters of reactive elements in the mathematical model (inductances and capacitances). A linearized system of steady-state equations (1) describes relations between currents and voltages in the circuit shown in fig. 2:

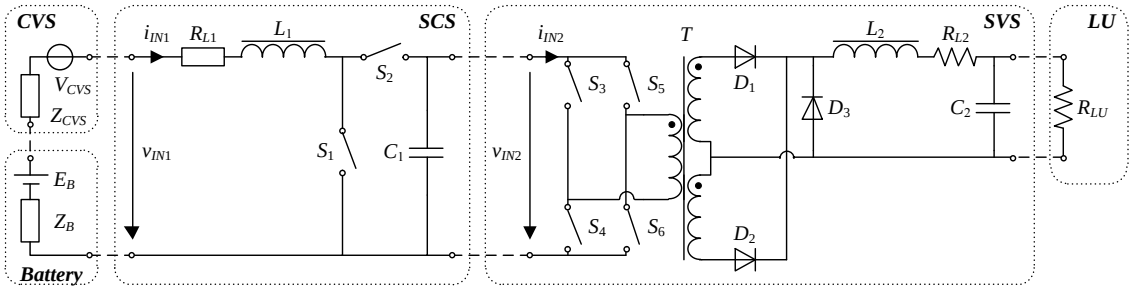

Figure 2. Equivalent electrical circuit of the CDU power part

$$\begin{cases} V_S = V_{CVS} + E_B \\ v_{IN1} = V_S - i_{IN1}(R_{CVS} + R_B) \\ i_{IN1} = I_{IN1}D_I + I_{IN1}d_i + i_{in1}D_I + i_{IN2} \\ v_{IN2} = v_{IN1} - i_{IN1}R_{L1} + V_{IN2}D_I + v_{in2}D_I + V_{IN2}d_i \\ i_{IN2} = (I_{LU}D_V + i_{lu}D_V + I_{LU}d_v)n \\ v_{LU} = (V_{IN2}D_V + v_{in2}D_V + V_{IN2}d_v)n - i_{LU}R_{L2} \\ i_{LU} = v_{LU}G_{LU} \end{cases}, \quad (1)$$

where V_S – voltage of the source, V_{CVS} – dc voltage at CVS output, E_B – battery cell dc voltage, v_{IN1} –SCS input voltage, $i_{IN1} = I_{IN1} + i_{in1}$ – total value of SCS input current, I_{IN1} – equilibrium point value of i_{IN1}, i_{in1} – variation of i_{IN1}, R_{CVS} – CVS resistance, R_B – battery cell resistance, $d_I = D_I + d_i$ – total value of SCS duty cycle, D_I – equilibrium point value of d_I, d_i – variation of d_I, i_{IN2} – SVS input current, $v_{IN2} = V_{IN2} + v_{in2}$ – total value of SVS input voltage, V_{IN2} – equilibrium point value of v_{IN2}, v_{in2} – variation of v_{IN2}, R_{L1} – resistance of L_1, i_{IN2} – SVS input current, $i_{LU} = I_{LU} + i_{lu}$ – total value of LU current, I_{LU} – equilibrium point value of i_{LU}, i_{lu} – variation of i_{LU}, $d_V = D_V + d_v$ – total value of SVS duty cycle, D_V – equilibrium point value of d_V, d_v – variation of d_V, n – turns ratio of transformer T, v_{LU} – LU voltage, R_{L2} – resistance of L_2, G_{LU} – conductance of LU.

The system of equations (2) describes a control system of CDU. Along with (1), it forms a mathematical model of CDU. Block diagram of total model (fig. 3) consists of systems (1) and (2):

$$\begin{cases} d_I = (V_{REFI} - i_{IN1}K_{CS})K_I K_{PWMI} \\ d_V = (v_{IN2}K_{VS} - V_{REFV})K_V K_{PWMV} \end{cases}, \quad (2)$$

where V_{REFI} – reference voltage of SCS feedback loop, K_{CS} – current sensor gain, K_I – gain of SCS feedback loop, K_{PWMI} – gain of SCS pulse width modulator (PWM), V_{REFV} – reference

voltage of SVS feedback, K_{VS} – voltage sensor gain, K_V – gain of SVS feedback loop, K_{PWMV} – gain of SVS PWM.

Expressions for the current and voltage with offset that appeared as a result of the presence of steady-state error were obtained from systems (1) and (2):

$$i_{IN1} = f(V_S, V_{REFI}, V_{REFV}, K_I, K_V), \tag{3}$$

$$v_{IN2} = f(V_S, V_{REFI}, V_{REFV}, K_I, K_V). \tag{4}$$

Open-loop transfer functions of SCS and SVS control loops at steady state become SCS gain KOLI and SVS gain KOLV, respectively, which are functions of the following variables:

$$K_{OLI} = f(V_S, V_{REFI}, V_{REFV}, K_I, K_V), \tag{5}$$

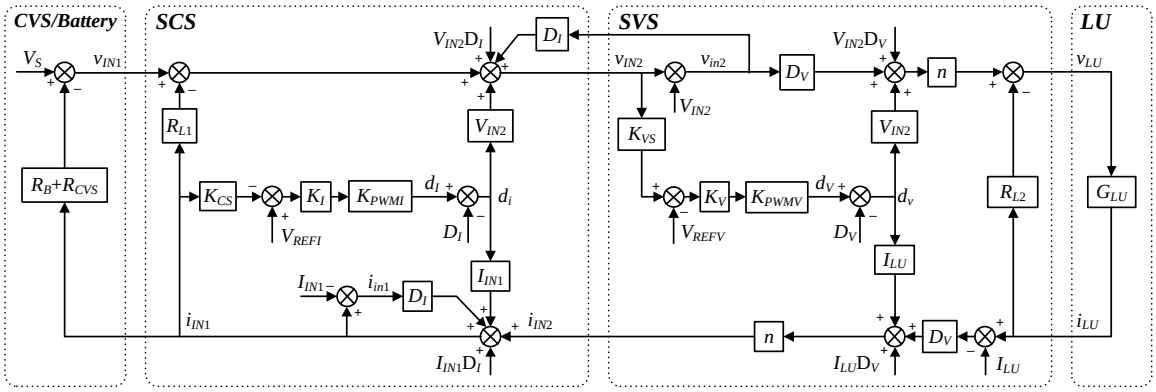

Figure 3. Block diagram of linearized CDU model for steady-state conditions

$$K_{OLV} = f(V_S, V_{REFI}, V_{REFV}, K_I, K_V). \tag{6}$$

Since the CDU input current varies in a wide range of values down to zero, usage of the standard relative error for evaluation of the system accuracy will give to large errors at low currents. Percentage error normalized relative to maximum measurement value (hereinafter – percentage error, designated as δ_M) is more convenient for evaluation purposes [17–18]. The percent error of SCS control loop δ_{MI} is used for SCS input current stabilization accuracy estimation:

$$\delta_{MI} = \left| \frac{I_{IN1} - i_{IN1}}{I_{IN1\max}} \right|, \tag{7}$$

where $i_{IN1} = I_{IN1} + i_{in1}$ – total value of SCS input current, I_{IN1} – equilibrium point value of i_{IN1}, I_{IN1max} – the maximum current of the CDU (I_{IN1max} = 160 A).

SCS percentage error δ_{MI} for the CDU was set to 0.5%.

The percent error of SVS control loop δ_{MV} is similarly used for SVS input voltage stabilization accuracy estimation:

$$\delta_{MV} = \left| \frac{V_{IN2} - v_{IN2}}{V_{IN2\max}} \right|, \tag{8}$$

where $v_{IN2} = V_{IN2} + v_{in2}$ – total value of SVS input voltage, V_{IN2} – equilibrium point value of v_{IN2}, V_{IN2max} – the maximum input voltage of SVS.

4. Simulation and experimental results

Study the impact of various operational modes of the CDU on the SCS current percentage error allows determining the device parameters that ensure the required accuracy of the CDU input current stabilization. Modes of operation of the CDU are defined by different values of the following quantities: the input current I_{IN1}, voltage of the source V_S, SCS gain K_{OLI} and SVS gain K_{OLV}.

Equations (3)-(8) allow obtaining the implicit dependence of SCS δ_{MI} and SVS δ_{MV} percentage errors from SCS K_{OLI} and SVS K_{OLV} gains (fig.4-9).

Figures 4 and 5 show that with an increase in SCS gain K_{OLI} value of SCS percentage error δ_{MI} decreases, regardless of the action of various destabilizing factors.

Figure 6 shows that SCS percentage error δ_{MI} remains practically constant with increasing of SVS gain K_{OLV} and decreases with increasing of SCS gain K_{OLI}.

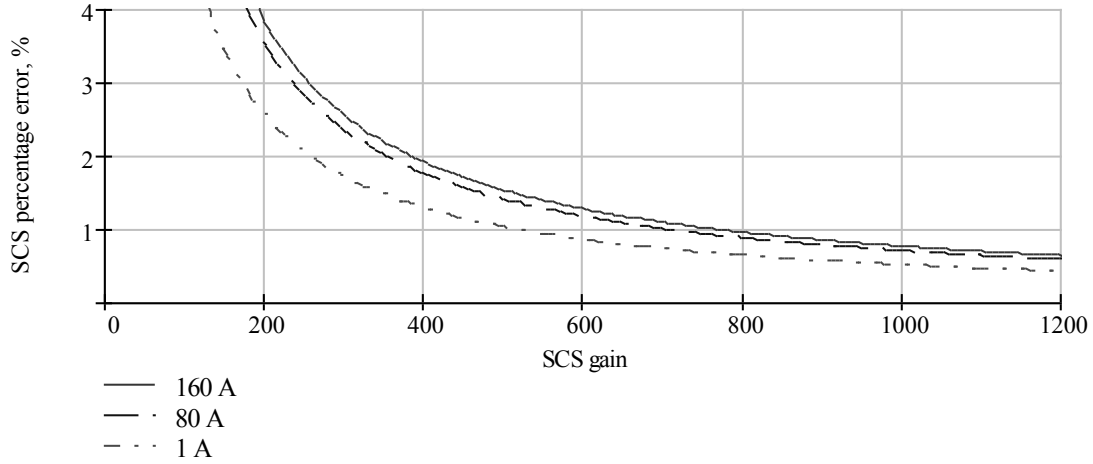

Figure 4. An implicit relation between SCS percentage error δ_{MI} error and SCS gain K_{OLI} for different values of the input current I_{IN1}

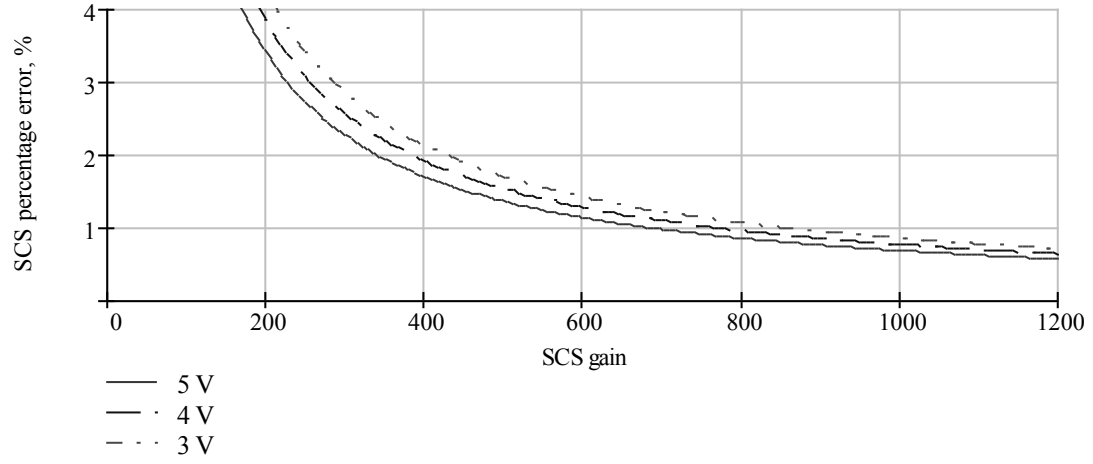

Figure 5. An implicit relation between SCS percentage error δ_{MI} and SCS gain K_{OLI} for different values of the input voltage V_S

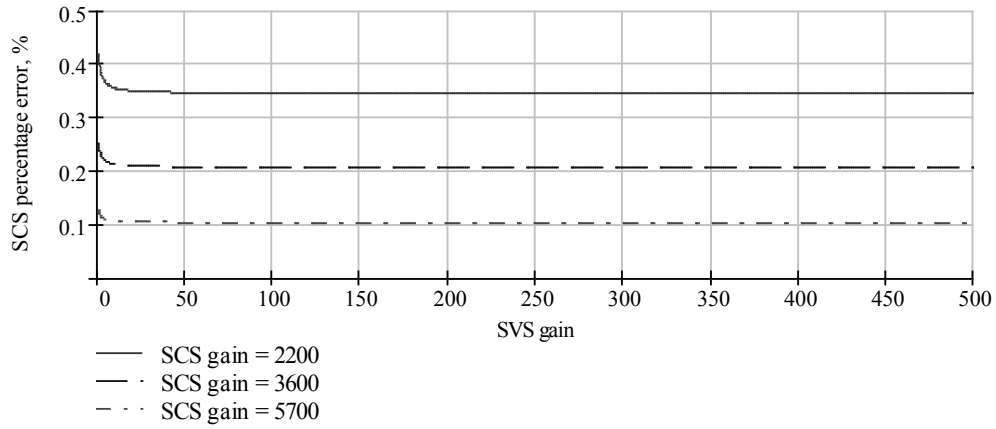

Figure 6. An implicit relation between SCS percentage error δ_{MI} and SVS gain K_{OLV} for different values of SCS gain K_{OLI}

The value of SVS gain K_{OLV} determines the SVS percentage error δ_{MV}. It was established experimentally that for the normal CDU operation a value of SVS percentage error δ_{MV} should be 3-5% over the entire range of input voltages and currents. Figures 7-9 show that to ensure this requirement is necessary that the value of SVS gain K_{OLV} was big enough.

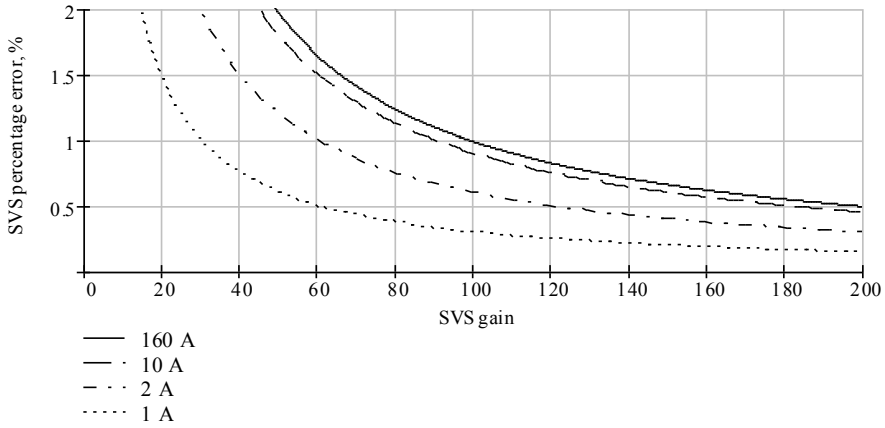

Figure 7. An implicit relation between SVS percentage error δ_{MV} and SVS gain K_{OLV} for different values of the input current I_{IN1}

Figures 7 and 8 show that SVS percentage error δ_{MV} decreases with increasing SVS gain K_{OLV} and does not depend on the input voltage V_S.

Figure 9 shows that SVS percentage error δ_{MV} significantly depends on SCS gain K_{OLI} and the input current I_{IN1}, which imposes restrictions on the minimum value of SCS gain K_{OLI}.

It can be concluded from the results of mathematical modeling that SCS gain K_{OLI} and SVS gain K_{OLV} are interrelated. It is methodically reasonable to select the value of SVS gain K_{OLV} first and then to select large enough SCS gain K_{OLI}.

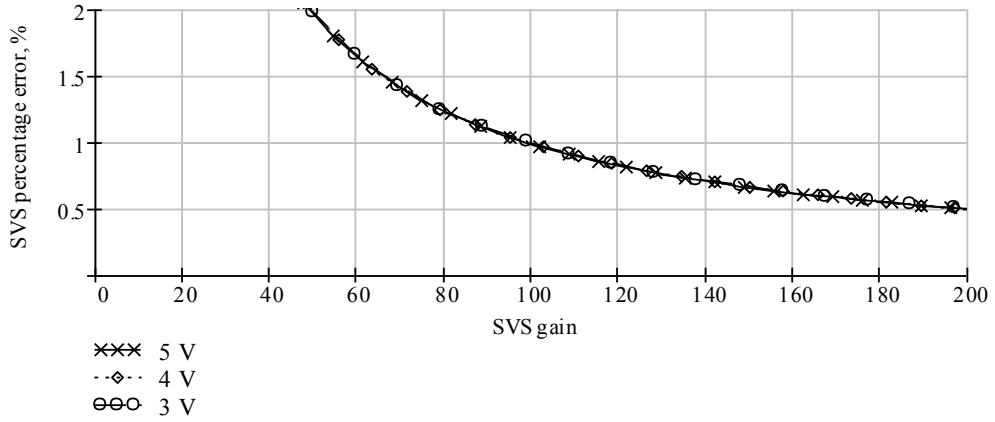

Figure 8. An implicit relation between SVS percentage error δ_{MV} and SVS gain K_{OLV} for different values of the input voltage V_S

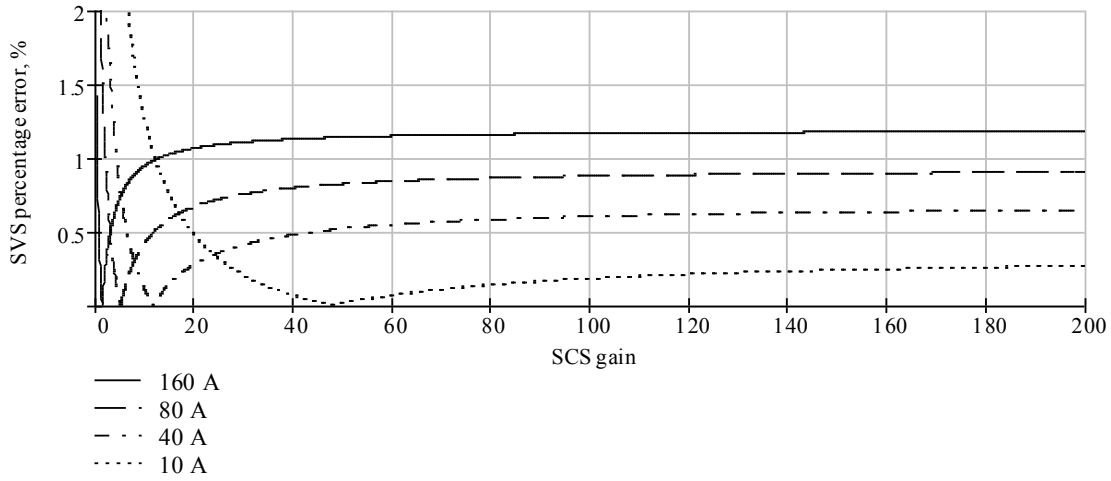

Figure 9. An implicit relation between SVS percentage error δ_{MV} and SCS gain K_{OLI} for different values of the input current I_{IN1}

The required accuracy of attribute stabilization was also achieved by increasing system type by least 1 through the introduction of the digital integrator in the SCS control loop [19].

A difference equation of the digital integrator is of the form:

$$E_g[n] = k \cdot E_g[n] + E_g[n-1], \tag{9}$$

where n – unitless time, k – integration ratio.

To illustrate the correctness of the developed approach for CDU parameters, experimental studies of SCS percentage error for LISP-85 Li-ion battery [20] were performed (fig. 10).

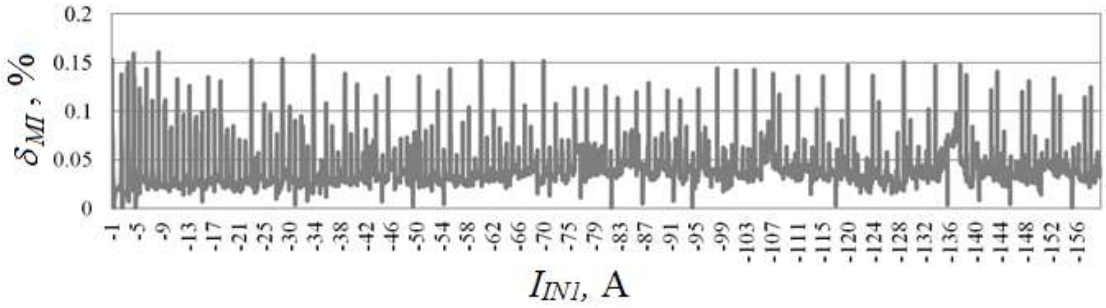

Figure 10. Experimental relation between SCS percentage error δ_{MI} and depending on input current I_{IN1}

The experimental results confirm that the SCS percentage error does not exceed 0.2%, which is consistent with the selected design conditions (δ_{MI} = 0.5%).

5. Conclusion

The proposed approach to the selection of the CDU parameters provides the desired percentage errors of required attributes of Li-ion battery operational modes. SCS gain K_{OLI} and SVS gain K_{OLV} are interrelated, which can be confirmed by the results of mathematical modelling. For this reason, it makes sense to select the value of SVS gain K_{OLV} first and then to select large enough SCS gain K_{OLI}. The required accuracy of attribute stabilization was also achieved by increasing system type by least 1 through the introduction of the digital integrator in the SCS control loop.

Acknowledgements

This study was supported by the Ministry of Education and Science of the Russian Federation (Government Contract 14.577.21.0082, unique identifier RFMEFI57714X0082).

References

[1] Yang F Y, Xing Y, Wang D, Tsui K-L 2016 A comparative study of three model-based algorithms for estimating state-of-charge of lithium-ion batteries under a new combined dynamic loading profile *Applied Energy* vol **164** pp 387–399 doi: 10.1016/j.apenergy.2015.11.072

[2] Hussein A A 2015 Capacity Fade Estimation in Electric Vehicle Li-Ion Batteries Using Artificial Neural Networks *IEEE Trans. on Industry Applications* vol **51** No. 3 pp 2321–2330 doi: 10.1109/TIA.2014.2365152

[3] Xing Y, He W, Pecht M, Tsui K L 2014State of charge estimation of lithium-ion batteries using the open-circuit voltage at various ambient temperatures *Applied Energy* vol **113** pp 106–115 doi: 10.1016/j.apenergy.2013.07.008

[4] Sight H N 2009 Lithium-ion battery prognostic testing and process. Patent US, No. 7576545 B2,

[5] Kwok W Y 2001 Method of calculating dynamic state-of-charge within a battery. Patent US, No. 6300763 B1

[6] Guiheen J V, Sight H, Palanisamy T G 2003 Method and apparatus for determining the state of charge of a lithium-ion battery. Patent US, No. 6586130 B1

[7] Sayfang G R 1990 Battery state of charge indicator. Patent US, No. 4949046 A

[8] Palanisamy T, Sight H, Atehortua H, Hoenig S 2005 Method and apparatus for determining the available of energy of a lithium ion battery. Patent US, No. 20050269993 A1
[9] Chroma Systems Solutions, Inc. 17011 Programmable Charge/Discharge Tester. Available at: http://www.chromausa.com/product/17011-programmable-chargedischarge-tester/ (accessed 01.02.2017)
[10] Cadex Electronics Inc. C8000 BATTERY TESTING SYSTEM. Available at: http://www.cadex.com/en/products/c8000-battery-testing-system/ (accessed 01.02.2017)
[11] Kopylov E A, Mizrah E A, Fedchenko A S, Lobanov D K 2016Study of a lithium-ion battery charge-discharge test unit characteristics *IOP Conf. Series: Materials Science and Engineering* vol **122** doi: 10.1088/1757-899X/122/1/012015
[12] Fedchenko A S, Kopylov E A, Lobanov D K, Mizrah E A 2016 Static accuracy of the automated stand for lithiumion batteries testing *18th Mediterranean Electrotechnical Conference (MELECON)*, Lemesos doi: 10.1109/MELCON.2016.7495336
[13] Gu B, Lai J-S, Kees N, Zheng C 2013 Hybrid-Switching Full-Bridge DC–DC Converter With Minimal Voltage Stress of Bridge Rectifier, Reduced Circulating Losses, and Filter Requirement for Electric Vehicle Battery Chargers *IEEE Trans. on Power Electronics* vol **28** No. 3 pp 1132–1144 doi: 10.1109/TPEL.2012.2210565
[14] Gautam D ., Musavi F, Eberle W, Dunford W G 2013 A Zero-Voltage Switching Full-Bridge DC--DC Converter With Capacitive Output Filter for Plug-In Hybrid Electric Vehicle Battery Charging *IEEE Trans. on Power Electronics* vol **28** No. 12 pp 5728–5735 doi: 10.1109/TPEL.2013.2249671
[15] GOST R MEK 62660-1-2014. Akkumulyatory litiy-ionnye dlya elektricheskikh dorozhnykh transportnykh sredstv. Chast' 1. Opredelenie rabochikh kharakteristik. [IEC 62660-1:2010. Secondary lithium-ion cells for the propulsion of electric road vehicles. Part 1. Performance testing]. Moscow, Standartinform Publ., 2015. 34 p.
[16] National Instruments Corporation PXIe-4300. Available at: http://www.ni.com/ru-ru/support/model.pxie-4300.html (accessed 01.02.2017)
[17] Mizrah E A 2001 Method for assessing the accuracy of spacecraft primary energy source simulators *Vestnik SibGAU* vol **8** No. 2 pp 10–14 (In Russ.)
[18] Mizrah E A 2005 The analysis of static accuracy of solar batteries simulators *Vestnik SibGAU* vol **12** No. 4 pp 24–27 (In Russ.)
[19] Selvaraj J, Rahim N A 2008 Multilevel Inverter For Grid-Connected PV System Employing Digital PI Controller *IEEE Trans. on Industrial Electronics* vol **56** No. 1 pp 149–158 doi: 10.1109/TIE.2008.928116
[20] JSC «Saturn» LISP-85. Available at: http://www.saturn.kuban.ru/liab_spec.html (accessed 01.02.2017)